**Coupled Systems Mechanics,** *Vol. 13, No. 6 (2024) 529-546*
https://doi.org/10.12989/csm.2024.13.6.529


# Analysis of wave propagation in micropolar thermoelastic media incorporating hyperbolic two temperature effects with framework of modified Green-Lindsay theory

Sachin Kaushal*[1], Indu Bala[1], Magdy A. Ezzat[2], Nidhi Arora[3] and Ashok Sharma[4]

*[1]Department of Mathematics, School of Chemical Engineering and Physical Sciences, Lovely Professional University, Phagwara, India*
*[2]Department of Mathematics, Faculty of Science, Qassim University, Buraydah, 51452, Saudi Arabia*
*[3]Department of Computer Science and Engineering, Lovely Professional University, 144411, Phagwara, India*
*[4]Department of Computer Science and IT, University of Jammu, Jammu and Kashmir, India*

*(Received September 15, 2024, Revised December 16, 2024, Accepted December 17, 2024)*

**Abstract.** The study examines the behaviour of waves propagating through a homogeneous, isotropic thermoelastic medium under modified micropolar Green-Lindsay (MMG-L) model along with hyperbolic two-temperature (HTT) parameter. The governing Eqs. are formulated and explained after reducing to two dimension and a dimensionless form. Amplitude ratios are obtained for various waves namely Longitudinal waves (LD-wave), Transverse wave (T-wave), Coupled Displacement-I wave (CD-I wave) and Coupled Displacement-II wave (CD-II wave), for the considered model. This article distinctively explores the influence of the HTT parameter on wave propagation within the modified Green-Lindsay (MG-L) model. Amplitude ratios are presented graphically to depict the influence of HTT parameter along with different models of thermoelasticity namely the MG-L and Green-Lindsay (G-L) model. Also, the graphically presented results shows the potential applications in geophysics, seismology and earthquake engineering providing valuable insights into wave interaction dynamics within micro-structured materials. Some special cases are also deduced from the present investigation.

**Keywords:** amplitude ratio; hyperbolic two-temperature; micropolar thermoelastic; modified Green-Lindsay

## 1. Introduction

A rigid body deforms under external forces, altering the shape, volume or length while an elastic body regains its original state. Theory of thermoelasticity explores the relationship between heat and the mechanical energy of a body. The shortcoming of classical theory (CT) theory are addressed by two generalized theories of thermoelasticity presented by Lord and Shulman (L-S) (1967) and Green-Lindsay (G-L) (1972). Youssef (2006) proposed a new theory of generalized thermoelasticity, incorporating heat conduction in deformable bodies governed by two distinct

---

*Corresponding author, Ph.D., E-mail: sachin_kuk@yahoo.co.in


http://www.techno-press.org/?journal=csm&subpage=8 ISSN: 2234-2184 (Print), 2234-2192 (Online)

temperatures: conductive and thermodynamic. Ezzat *et al.* (2012) constructed a mathematical model for TT magneto-thermoelasticity, by incorporating the fractional-order dual-phase-lag heat conduction law. Ezzat *et al.* (2018) presented a mathematical model for the TT phase-lag Green-Nagdhi thermoelasticity theory. Various authors have explored different problems, with notable contributions including (Ezzat 1995, Ezzat 2004, Abo-Dahab and Lofty 2015, Lofty 2012, Vlase *et al.* 2017, Lofty *et al.* 2019).

Youssef and Bary (2018) introduced an HTT generalized thermoelastic model. Kumar *et al.* (2020) described thermoelastic interactions in an infinite elastic medium with a cylindrical cavity in the context of HTT parameter.

El-Bary (2021) developed a mathematical model of HTT generalized thermoelasticity combined with the fractional stress theory for a homogeneous isotropic solid cylindrical infinite medium. Lofty *et al.* (2021) investigated the general solutions to a 1D problem for propagating waves in a generalized piezo-photo-thermoelastic medium using the HTT theory of thermoelastcitiy. Within the framework of the HTT generalized theory of thermoelasticity, Youssef and Lehaibi (2022) presented a two-dimensional model for a homogeneous and isotropic thermoelastic solid cylinder subjected to thermal shock.

In Eringen (1966), Tauchert *et al.* (1968), Eringen (1970), developed the linear and non-linear theory of micropolar thermoelasticity respectively. El-Karamany and Ezzat (2004) provided a formulation to the boundary integral Eq. method for a generalized linear micropolar thermoelastic model. Ezzat and Awad (2009) introduced modifications to Ohm’s law and the generalized Fourier’s law in the equations. of the linear theory of micropolar generalized magneto-thermoelasticity. Marin *et al.* (2020) investigated some results for the Moore-Gibson-Thompson (MG-T) theory of thermoelasticity of dipolar bodies. Abouelregal *et al.* (2022) investigated the effects of plane waves on materials with microstructures, based on micropolar thermoelasticity, including TT and higher order time derivatives. Sherief and Hussein (2023) enhanced a generalized micropolar theory of thermoelasticity by incorporating a fractional order model. Lofty and his co-authors discussed various types of problems, notable of them are (2015, 2020, 2021a, 2021b).

Yu *et al.* (2018) introduced strain rate into the G-L thermoelastic model, establishing a generalized thermoelastic framework. Subsequently, Quintanilla (2018) modified the theory proposed by Yu *et al.* on the G-L model. Sarkar and Mondal (2020) further enhanced the MG-L generalized thermoelastic model by incorporating the TT parameter and examined the reflection and propagation of thermoelastic plane waves in a homogeneous, isotropic thermally conducting elastic half-space with a stress-free and thermally insulated surface**.** Kumar *et al.* (2022) conducted a study to estimate the response of impedance parameters in a micropolar medium with the MMG-L generalized thermoelastic model. Using the MG-L generalized theory of thermoelasticity, Kaushal *et al.* (2023) analyzed the effects of non-local and HTT parameters in generalized thermoelastic medium under the MG-L model.

We consider a homogeneous, isotropic generalized thermoelastic micropolar medium within the framework of the MG-L theory of thermoelasticity. The primary focus of this research is to examine the impact of the HTT parameter on the amplitude ratio of the waves, namely the LD-wave, T-wave, CD-I wave and CD-II wave, in a homogeneous isotropic MMG-L medium. In section 3, the new set of governing Eqs. is reduced to a two-dimensional form and transformed into dimensionless quantities. In section 4, the eqations are solved using reflection technique, followed by stress-free boundary conditions given in section 5. Certain cases of interest are derived in section 6. Section 7 presents the numerical findings and graphical representations of the results, highlighting the impact of HTT and different theories of thermoelasticity. Finally, in section 8, the graphical findings are summarized. The physical context of the problem is related to geophysics, seismology and earthquake engineering research.

## 2. Basic equations

The field equations and constitutive relations in absence of body forces, body couples, and heat source (Eringen 1966, Yu *et al.* 2018, Youssef 2006) are defined as follows

$$\left(1+\eta_1\tau_1\frac{\partial}{\partial t}\right)[(\lambda+\mu)\nabla(\nabla.\vec{u})+(\mu+k)\nabla^2\vec{u}+k(\nabla\times\vec{\varphi})]-\left(1+\eta_2\tau_1\frac{\partial}{\partial t}\right)\gamma_1\nabla T=\rho\frac{\partial^2\vec{u}}{\partial t^2} \quad (1)$$

$$\gamma\nabla^2\vec{\varphi}+(\alpha+\beta)\nabla(\nabla.\vec{\varphi})+k[(\nabla\times\vec{u})-2\vec{\varphi}]=\rho j\frac{\partial^2\vec{\varphi}}{\partial t^2}, \quad (2)$$

$$K^*\nabla^2\phi=\rho C_e\left(1+\eta_3\tau_0\frac{\partial}{\partial t}\right)\frac{\partial T}{\partial t}+\left(1+\eta_4\tau_0\frac{\partial}{\partial t}\right)\gamma_1 T_0\dot{u}_{r,r}, \quad (3)$$

$$t_{pq}=\left(1+\eta_1\tau_1\frac{\partial}{\partial t}\right)\left[\lambda u_{r,r}\delta_{pq}+\mu\left(u_{p,q}+u_{q,p}\right)+k\left(u_{q,p}-\xi_{pqr}\varphi_r\right)\right]-\gamma_1\left(1+\eta_2\tau_1\frac{\partial}{\partial t}\right)T\delta_{pq}, \quad (4)$$

$$m_{pq}=\alpha\varphi_{r,r}\delta_{pq}+\beta\varphi_{p,q}+\gamma\varphi_{q,p}, \quad (5)$$

$$T=(1-a\nabla^2)\phi, \quad (6)$$

$$\ddot{T}=\ddot{\phi}-\beta^*\nabla^2\phi, \quad (7)$$

where $\lambda,\mu$ -Lame's constants, $\gamma_1=(3\lambda+2\mu+k)\alpha_t$, $\alpha_t$ -the coefficient of linear thermal expansion, $\vec{\varphi}$ -microrotation vector, $j$ -microinertia, $\vec{u}$ -displacement vector, $K^*$ -thermal conductivity, $\nabla^2$ -Laplacian operator, $\rho, C_e$ -density and specific heat, $T_0$ -reference temperature, $\delta_{pq}$-Kronecker delta, $\alpha,\beta\ \gamma,k$-micropolar constants, $\xi_{pqr}$-alternating tensor, $m_{pq}$-components of couple stress tensor, $t$ -time, $T$ -thermodynamic temperature, $\phi$ -conductive temperature, $t_{pq}$-components of stress tensor, $\tau_0,\tau_1$- the relaxation times, $\eta_1,\eta_2,\eta_3,\eta_4$-constants.

The Eqs. (1)- (7) reduce to the following

$\eta_1=\eta_2=\eta_3=\eta_4=1$, Modified Green-Lindsay (MG-L) (2018),
$\eta_1=\eta_4=0$, $\eta_2=\eta_3=1$, Green-Lindsay, (G-L) (1972),
$\eta_1=\eta_2=0$, $\eta_3=\eta_4=1$, Lord -Shulman, (L-S) (1967),
$\eta_1=\eta_2=\eta_3=\eta_4=0$, Coupled thermoelasticity, (C-T) (1980).

## 3. Problem statement

We consider a homogeneous and isotropic MMG-L half-space using a rectangular cartesian co-ordinate system $Ox_1x_2x_3$ having origin at $x_3=0$, along with $x_3$-axis pointing normally into the medium. We consider thermoelastic plane wave in $x_1,x_3$-plane with wave front paraller to $x_2$-axis and all the field variables depends only on $x_1,x_3$ and $t$.

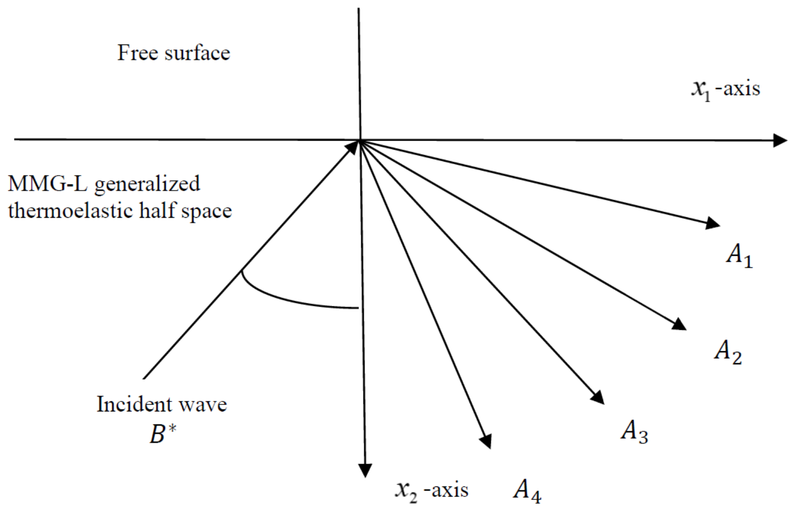


Fig. 1 Geometry of the problem

For two dimensional problems, we take the components of displacement and microrotation vector as

$$\vec{u} = (u_1, 0, u_3),\ \vec{\varphi} = (0, \varphi_2, 0). \tag{8}$$

The following dimensionless quantities are defined

$$\begin{gathered}(x_i', u_i') = \frac{\omega_1}{c_1}(x_i, u_i),\ t_{3i}' = \frac{t_{3i}}{\beta_1 T_0},\ (\phi', T') = \frac{1}{T_0}(\phi, T),\\ (t', \tau_0', \tau_1') = \omega_1(t, \tau_0, \tau_1),\ \varphi_2' = \frac{\rho C_1^2}{\gamma_1 T_0}\varphi_2,\ a' = \frac{\omega_1^2}{c_1^2}a,\\ m_{32}' = \frac{\omega_1}{\gamma_1 c_1 T_0}m_{32},\ \beta^{*\prime} = \frac{1}{c_1^2}\beta^*,\ (i = 1, 3)\end{gathered} \tag{9}$$

where

$$c_1^2 = \frac{\lambda + 2\mu + k}{\rho} \text{ and } \omega_1 = \frac{\rho C_e c_1^2}{K^*}.$$

After removing the primes and introducing the values defined by Eq. (9) along with Eq. (8), in Eqs. (1)-(7), we get

$$\left(1 + \eta_1\tau_1\frac{\partial}{\partial t}\right)\left[a_1\frac{\partial e}{\partial x_1} + a_2\nabla^2 u_1 - a_3\frac{\partial\varphi_2}{\partial x_3}\right] - a_4\left(1 + \eta_2\tau_1\frac{\partial}{\partial t}\right)\frac{\partial T}{\partial x_1} = \frac{\partial^2 u_1}{\partial t^2}, \tag{10}$$

$$\left(1 + \eta_1\tau_1\frac{\partial}{\partial t}\right)\left[a_1\frac{\partial e}{\partial x_3} + a_2\nabla^2 u_3 + a_3\frac{\partial\varphi_2}{\partial x_1}\right] - a_4\left(1 + \eta_2\tau_1\frac{\partial}{\partial t}\right)\frac{\partial T}{\partial x_3} = \frac{\partial^2 u_3}{\partial t^2}, \tag{11}$$

$$a_5\nabla^2\varphi_2 + a_6\left(\frac{\partial u_1}{\partial x_3} - \frac{\partial u_3}{\partial x_1}\right) - a_7\varphi_2 = \frac{\partial^2\varphi_2}{\partial t^2}, \tag{12}$$

$$\nabla^2\phi = \left(1 + \eta_3\tau_0\frac{\partial}{\partial t}\right)\frac{\partial T}{\partial t} + a_8\left(1 + \eta_4\tau_0\frac{\partial}{\partial t}\right)\frac{\partial e}{\partial t}, \tag{13}$$

$$t_{33} = \left(1 + \eta_1\tau_1\frac{\partial}{\partial t}\right)\left[a_{12}\left(\frac{\partial u_3}{\partial x_3}\right) + a_{13}\left(\frac{\partial u_1}{\partial x_1}\right)\right] - \left(1 + \eta_2\tau_1\frac{\partial}{\partial t}\right)T, \tag{14}$$

$$t_{31} = \left(1 + \eta_1\tau_1 \frac{\partial}{\partial t}\right)\left[a_9\left(\frac{\partial u_1}{\partial x_3}\right) + a_{10}\left(\frac{\partial u_3}{\partial x_1}\right) - a_{11}\varphi_2\right], \tag{15}$$

$$m_{32} = a_{14}\frac{\partial \varphi_2}{\partial x_3}, \tag{16}$$

$$T = (1 - a\nabla^2)\phi, \tag{17}$$

$$\ddot{T} = \ddot{\phi} - \beta^*\nabla^2\phi, \tag{18}$$

where $a_i's$ are defined as

$$a_1 = \frac{\lambda+\mu}{\rho c_1^2},\ a_2 = \frac{\mu+k}{\rho c_1^2},\ a_3 = \frac{\gamma_1 k T_0}{\rho^2 c_1^4},$$
$$a_4 = \frac{\gamma_1 T_0}{\rho c_1^2},\ a_5 = \frac{\gamma}{j\rho c_1^2},\ a_6 = \frac{k c_1^2}{j\gamma_1\omega_1^2 T_0},$$
$$a_7 = \frac{2k}{j\rho\omega_1^2},\ a_8 = \frac{\gamma_1 c_1^2}{K^*\omega_1},\ a_9 = \frac{\mu+k}{\gamma_1 T_0},$$
$$a_{10} = \frac{\mu}{\gamma_1 T_0},\ a_{11} = \frac{k}{\rho c_1^2},\ a_{12} = \frac{\lambda+2\mu+k}{\gamma_1 T_0},$$
$$a_{13} = \frac{\lambda}{\gamma_1 T_0},\ a_{14} = \frac{\gamma\omega_1^2}{\rho c_1^4},\ e = \frac{\partial u_1}{\partial x_1} + \frac{\partial u_3}{\partial x_3},$$
$$\nabla^2 = \frac{\partial^2}{\partial x_1^2} + \frac{\partial^2}{\partial x_3^2}.$$

The above system of equations is decoupled by taking $u_1$ and $u_3$ in dimensionless form as

$$u_1 = q_{,1} - \psi_{,3},\ u_3 = q_{,3} + \psi_{,1}. \tag{19}$$

Using Eq. (19) in Eqs. (11)-(16), we get the following set of equations

$$\left(1 + \eta_1\tau_1\frac{\partial}{\partial t}\right)\nabla^2 q - a_4\left(1 + \eta_2\tau_1\frac{\partial}{\partial t}\right)T = \frac{\partial^2 q}{\partial t^2}, \tag{20}$$

$$\left(1 + \eta_1\tau_1\frac{\partial}{\partial t}\right)a_2\nabla^2\psi + a_3\left(1 + \eta_1\tau_1\frac{\partial}{\partial t}\right)\varphi_2 = \frac{\partial^2\psi}{\partial t^2}, \tag{21}$$

$$a_5\nabla^2\varphi_2 - a_6\nabla^2\psi - a_7\varphi_2 = \frac{\partial^2\varphi_2}{\partial t^2}, \tag{22}$$

$$\nabla^2\phi = \left(1 + \eta_3\tau_0\frac{\partial}{\partial t}\right)\frac{\partial T}{\partial t} + a_8\nabla^2\left(1 + \eta_4\tau_0\frac{\partial}{\partial t}\right)\frac{\partial q}{\partial t}, \tag{23}$$

$$t_{33} = \left(1 + \eta_1\tau_1\frac{\partial}{\partial t}\right)\left[a_{12}\left(\frac{\partial^2\psi}{\partial x_1\partial x_3} + \frac{\partial^2 q}{\partial x_3^2}\right) + a_{13}\left(\frac{\partial^2 q}{\partial x_1^2} - \frac{\partial^2\psi}{\partial x_1\partial x_3}\right)\right] - \left(1 + \eta_2\tau_1\frac{\partial}{\partial t}\right)T, \tag{24}$$

$$t_{31} = \left(1 + \eta_1\tau_1\frac{\partial}{\partial t}\right)\left[a_9\left(\frac{\partial^2 q}{\partial x_1\partial x_3} - \frac{\partial^2\psi}{\partial x_3^2}\right) + a_{10}\left(\frac{\partial^2\psi}{\partial x_1^2} + \frac{\partial^2 q}{\partial x_1\partial x_3}\right) - a_{11}\varphi_2\right], \tag{25}$$

$$m_{32} = a_{14}\frac{\partial\varphi_2}{\partial x_3}. \tag{26}$$

## 4. Solution of the problem

Assuming harmonic motion, the solution for $q, \phi, \psi$ and $\varphi_2$ is expressed as

$$(q, \phi, \psi, \varphi_2) = (\bar{q}, \bar{\phi}, \bar{\psi}, \overline{\varphi_2})e^{\iota k(x_1\sin\theta - x_3\cos\theta) + \iota\omega t}, \tag{27}$$

where $\iota$ is iota, $k$ denoted as wave number, $\omega$ is angular velocity and quantities such as $\bar{q}, \bar{\phi}, \bar{\psi}$ and $\overline{\varphi_2}$ are arbitrary constants. After substituting the values of $q, \phi, \psi$ and $\varphi_2$ in Eqs. (20)-(23) along with Eq. (17) and (18), we get

$$(\nu^4 + A_1\nu^2 + A_2)(\bar{\psi}, \overline{\varphi_2}) = 0, \tag{28}$$

$$(\nu^4 + B_1\nu^2 + B_2)(\bar{q}, \bar{\phi}) = 0, \tag{29}$$

where

$$A_1 = \frac{(a_3a_6 - a_2a_7 + a_2\omega^2)R_1 + a_5\omega^2}{a_7 - \omega^2}, A_2 = \frac{-a_2a_5R_1\omega^2}{a_7 - \omega^2},$$

$$B_1 = \frac{\omega - a_4a_8\iota R_2R_4 - \iota R_3(\beta^* + R_1)}{\iota R_3},$$

$$B_2 = \frac{\iota\beta^* R_1R_3 - \omega R_1 + a_4a_8\iota\beta^* R_2R_4}{\iota R_3},$$

$$R_1 = (1 + \eta_1\tau_1\iota\omega), R_2 = (1 + \eta_4\tau_0\iota\omega),$$

$$R_3 = (1 + \eta_3\tau_0\iota\omega), R_4 = (1 + \eta_2\tau_1\iota\omega).$$

## 5. Boundary conditions

At stress free surface, the boundary conditions are vanishing of stresses and temperature gradient, mathematically it can be written as

$$\text{(i) } t_{33} = 0, \text{ (ii) } t_{31} = 0, \text{ (iii) } m_{32} = 0, \text{ (iv) } \frac{\partial T}{\partial x_3} = 0, \text{ at } x_3 = 0. \tag{30}$$

To obtain the amplitude ratios, we consider $\bar{q}, \bar{\phi}, \bar{\psi}, \overline{\varphi_2}$ in the following form

$$\bar{q} = A_{0i}e^{\iota k_0(x_1 \sin\theta_0 - x_3\cos\theta_0) + \iota\omega t} + A_ie^{\iota k_i(x_1\sin\theta_i + x_3\cos\theta_i) + \iota\omega t}, \tag{31}$$

$$\bar{\phi} = d_iA_{0i}e^{\iota k_0(x_1 \sin\theta_0 - x_3\cos\theta_0) + \iota\omega t} + d_iA_ie^{\iota k_i(x_1\sin\theta_i + x_3\cos\theta_i) + \iota\omega t}, \tag{32}$$

$$\bar{\psi} = A_{0j}e^{\iota k_0(x_1 \sin\theta_0 - x_3\cos\theta_0) + \iota\omega t} + A_je^{\iota k_j(x_1\sin\theta_j + x_3\cos\theta_j) + \iota\omega t}, \tag{33}$$

$$\overline{\varphi_2} = f_iA_{0j}e^{\iota k_0(x_1 \sin\theta_0 - x_3\cos\theta_0) + \iota\omega t} + f_iA_je^{\iota k_j(x_1\sin\theta_j + x_3\cos\theta_j) + \iota\omega t}, \tag{34}$$

where $d_i = \frac{(\omega^2 - k_i^2)R_1}{a_4R_4\left(1 - \frac{\beta^* k_i^2}{\omega^2}\right)}, f_i = \frac{a_6k_i^2}{a_5k_i^2 + a_7 - \omega^2}, (i = 1{,}2), (j = 3{,}4).$

$A_{0i}(i = 1{,}2)$ are the amplitude of incident LD-wave, T-wave. $A_{0j}(j = 3{,}4)$ are the amplitude of CD-I wave and CD- II wave. $A_i$ $(i = 1{,}2)$ are the amplitude of the reflected LD-wave and reflected T-wave and $A_j$ $(j = 3{,}4)$ is the amplitude of the CD-I wave and CD- II wave.

Snell's Law is given as

$$\frac{\sin\theta_0}{v_0} = \frac{\sin\theta_1}{v_1} = \frac{\sin\theta_2}{v_2} = \frac{\sin\theta_3}{v_3} = \frac{\sin\theta_4}{v_4}, \tag{35}$$

where

$$k_1v_1 = k_2v_2 = k_3v_3 = k_4v_4 = \omega, \text{ at } x_3 = 0, \tag{36}$$

$$\upsilon_0 = \begin{cases} \nu_1, \text{for incident LD} - \text{wave} \\ \nu_2, \text{for incident T} - \text{wave} \\ \nu_3, \text{for incident CD} - \text{I wave} \\ \nu_4, \text{for incident CD} - \text{II wave} \end{cases}.$$

Using (31)-(34) along with (35)-(36) in the boundary conditions given by (30), we obtained a system of equations as

$$\sum a_{ij} Z_j = Y_i, (i, j = 1, 2, 3, 4), \quad (37)$$

$$a_{1i} = -R_1 k_i^2 [a_{12}\cos^2\theta_i + a_{13}\sin^2\theta_i] - R_4\left(1 - \frac{\beta^* k_i^2}{\omega^2}\right) d_i,$$
$$a_{1j} = R_1 k_j^2 \sin\theta_j \cos\theta_j\,(a_{13} - a_{12}),$$
$$a_{2i} = -R_1 \sin\theta_i \cos\theta_i\, k_i^2 (a_9 + a_{10}),$$
$$a_{2j} = a_9 R_1 \cos^2\theta_j\, k_j^2 - a_{10} R_1 \sin^2\theta_j\, k_j^2 - a_{11} f_i R_1,$$
$$a_{3j} = a_{14}\iota k_j f_i \cos\theta_j,\; a_{4i} = \left(1 - \frac{\beta^* k_i^2}{\omega^2}\right)\iota d_i k_i \cos\theta_i,$$
$$i = 1,2 \text{ and } j = 3,4$$
$$\text{and } Z_1 = \frac{A_1}{B^*}, Z_2 = \frac{A_2}{B^*}, Z_3 = \frac{A_3}{B^*}, Z_4 = \frac{A_4}{B^*}.$$

For incident LD-wave $B^* = A_{01}$

$$Y_1 = -a_{11}, Y_2 = a_{21}, Y_3 = a_{31}, Y_4 = a_{41}.$$

For incident T-wave $B^* = A_{02}$

$$Y_1 = -a_{12}, Y_2 = a_{22}, Y_3 = a_{32}, Y_4 = a_{42}.$$

For incident CD-I wave $B^* = A_{03}$

$$Y_1 = a_{13}, Y_2 = -a_{23}, Y_3 = a_{33}, Y_4 = a_{43}.$$

For incident CD-II wave $B^* = A_{04}$

$$Y_1 = a_{14}, Y_2 = -a_{24}, Y_3 = a_{34}, Y_4 = a_{44}.$$

## 6. Unique cases

### *6.1 Modified Green-Lindsay with Hyperbolic two-temperature*

When substituting $\alpha = \beta = \gamma = k = j = 0$ in Eq. (37), we get the results for the case of MG-L theory of thermoelasticity along with HTT parameter.

### *6.2 Green-Lindsay theory of thermoelasticity along with two-temperature parameter*

Putting $\eta_1 = \eta_4 = 0, \eta_2 = \eta_3 = 1, \beta^* = a$, reduces the system of equation defined by (37) for the case of G-L theory of micropolar thermoelasticity along with TT parameter, results tally with those obtained by Kumar *et al*. (2015).

### *6.3 Lord-Shulman theory of thermoelasticity with two-temperature parameter*

Let $\eta_1 = \eta_2 = 0$, $\eta_3 = \eta_4 = 1$, $\beta^* = a$, Eq. (37) will yield the expression for micropolar theory of thermoelasticity for L-S model along with TT parameter, results tally with those obtained by Kumar *et al*. (2015).

### *6.4 Green-Lindsay theory of thermoelasticity*

Taking $\eta_1 = \eta_4 = 0$, $\eta_2 = \eta_3 = 1$, $\beta^* = 0$, reduces the system of Eq. defined by (37) for micropolar theory of thermoelasticity for G-L model.

### *6.5 Lord-Shulman theory of thermoelasticity*

By taking $\eta_1 = \eta_2 = 0, \eta_3 = \eta_4 = 1,\ \beta^* = 0$, i.e. in the absence of TT parameter, Eq. (37) gives expression for micropolar theory of thermoelastic for L-S model.

## 7. Computational interpretation

A case of aluminium-epoxy material is being considered for numerical results and discussions and the values of relevant physical constants are given by Gauthier (1982):

(i) Micropolar parameters

$$\lambda = 7.59 \times 10^9 \mathrm{Nm}^{-2}, \mu = 1.89 \times 10^9 \mathrm{Nm}^{-2},$$
$$k = 0.0149 \times 10^9 \mathrm{Nm}^{-2}, \rho = 2.19 \times 10^3 \mathrm{Kgm}^{-3},$$
$$\gamma_1 = 2.68 \times 10^5 \mathrm{N}, C_e = 2.361 \times 10^{10} \mathrm{m}^2\mathrm{s}^{-2}\mathrm{K}^{-1},$$
$$j = 0.00196 \mathrm{m}^2.$$

(ii) Thermal parameters

$$T_0 = 296\mathrm{K}, \omega = 1\mathrm{Hz}, \tau_0 = 0.1\mathrm{s},$$
$$\tau_1 = 0.2\mathrm{s}, K^* = 2.04 \times 10^2 \mathrm{Jsec}^{-1}\mathrm{m}^{-1}\mathrm{deg}^{-1}.$$

We are considering four different cases. Two cases are for MMG-L, one is with HTT parameter and other is when HTT parameter is absent. Two cases are considered for micropolar theory of thermoelasticity with G-L model, one is with HTT parameter and second is when HTT parameter is absent.

In Fig. 2-17

**i. Solid black line** represents the case of MMG-L along with HTT parameter (HTMGL) when $\beta^* = 0.75$.

**ii**. **Solid black line with center symbol** '◊', represents the case of MG-L in the absence of HTT parameter (MGL) i.e., for $\beta^* = 0$.

**iii. Dashed blue line** represents the case of G-L theory of thermoelasticity with HTT parameter (HTGL) and $\beta^* = 0.75$.

**iv. Blue dashed line having center symbol as** 'Δ', represents the case of G-L theory of thermoelasticity (G-L) with $\beta^* = 0$ (i.e., the absence of HTT parameter).

**LD-WAVE**

Fig. 2 is plotted to describe $|Z_1|$ vs $\theta_0$. A significant decrease in magnitude of $|Z_1|$ is noticed in the range $0^0 \leq \theta_0 \leq 35^0$ for G-L model of thermoelasticity, while for MG-L model of thermoelasticity an increasing trend is noticed. The impact of HTT parameter is also visible as it enhances the amplitude ratio for both considered model of thermoelasticity.

Fig. 3 gives the graphical description of $|Z_2|$ vs $\theta_0$. It is noticed that value of $|Z_2|$ shows a descending behaviour and gradually diminishing towards zero for all the considered cases in the entire range. The HTT parameter increases the magnitude of $|Z_2|$ for both MG-L and G-L model of thermoelasticity which reveals the impact of HTT on amplitude ratio.

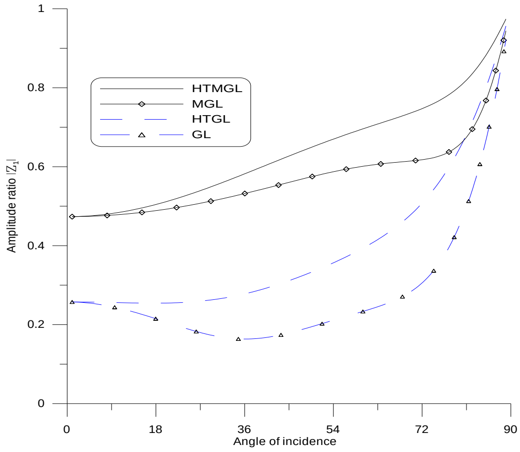


Fig. 2 Variation of amplitude ratio $|Z_1|$ for LD- wave

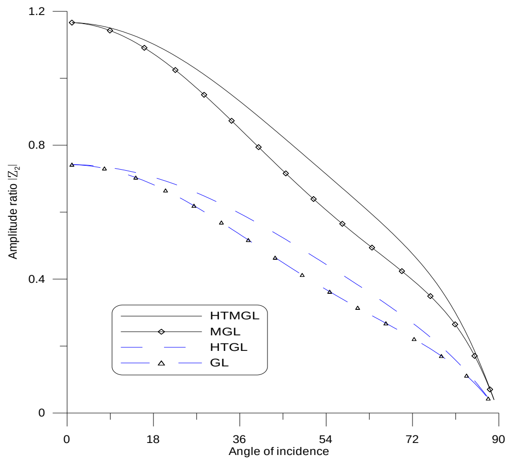


Fig. 3 Variation of amplitude ratio $|Z_2|$ for LD- wave

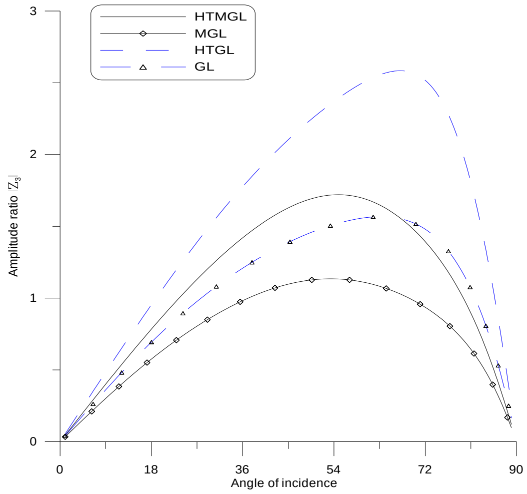


Fig. 4 Variation of amplitude ratio $|Z_3|$ for LD- wave

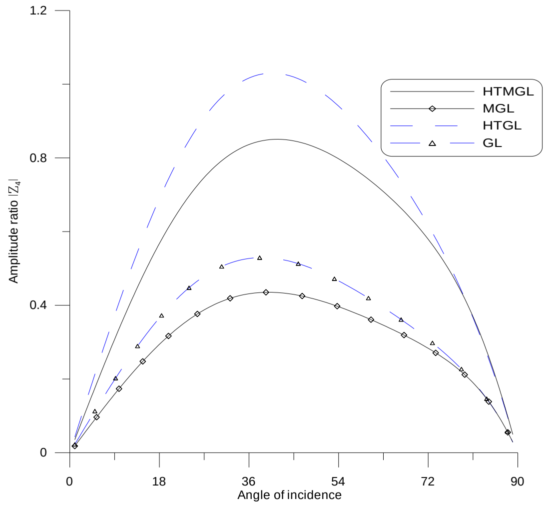


Fig. 5 Variation of amplitude ratio $|Z_4|$ for LD- wave

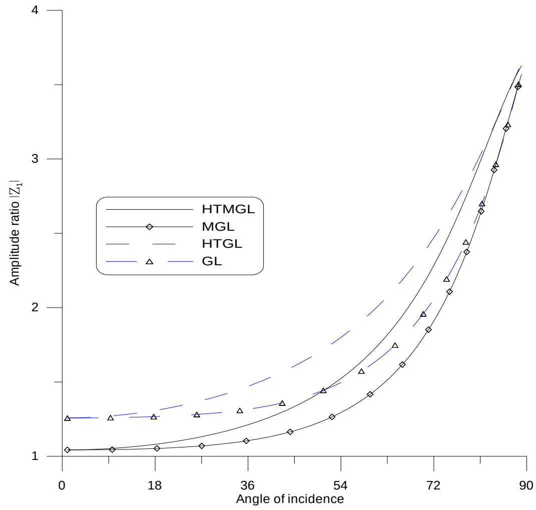


Fig. 6 Variation of amplitude ratio $|Z_1|$ for T- wave

Fig. 4 elucidates the impact of various theories of thermoelasticity on $|Z_3|$ vs $\theta_0$. It is observed that the value for $|Z_3|$ are greater for G-L model of thermoelasticity i.e., HTGL and GL in comparison to those observed for HTMGL and MGL respectively. It is also noticed that the value of $|Z_3|$ firstly increases and later on decrease for all the considered cases.

It is revealed from Fig. 5, which is a plot of $|Z_4|$ vs $\theta_0$, that the value of $|Z_4|$ shows ascending behaviour in $0^0 \leq \theta_0 \leq 45^0$ and later on decreases, with an increase in $\theta_0$. The highest of $|Z_4|$ is seen at $\theta = 45^0$ for HTGL.

**T-WAVE**

Fig. 6 depicts the variations of $|Z_1|$ vs $\theta_0$. A gradual increase in the first half of interval is seen and after $\theta = 45^0$, $|Z_1|$ shows a steep increase in magnitude for all the considered cases.

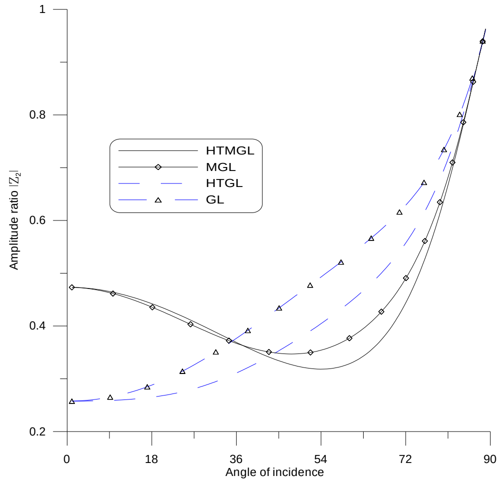


Fig. 7 Variation of amplitude ratio $|Z_2|$ for T- wave

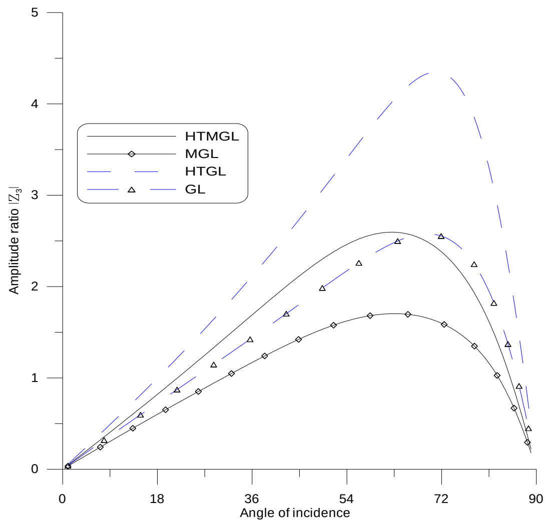


Fig. 8 Variation of amplitude ratio $|Z_3|$ for T- wave

It is depicted from Fig. 7 which is a plot of $|Z_2|$ vs $\theta_0$. It is noticed that $|Z_2|$ shows contrary behaviour for MG-L model (HTMGL, MGL) of thermoelasticity as observed for G-L model of thermoelasticity in the range $0^0 \leq \theta_0 \leq 45^0$.

Fig. 8 shows the variation of $|Z_3|$ vs $\theta_0$. It is seen that HTT parameter enhances the value of $|Z_3|$ for both theories of thermoelasticity. It is also observed that in case of HTMGL and MGL the values increase in the range from $0^0 \leq \theta_0 \leq 60^0$, whereas for the case of HTGL and GL the value of $|Z_3|$ increases in the range from $0^0 \leq \theta_0 \leq 70^0$ and later follows a downward trend for all considered cases.

Fig. 9 displays $|Z_4|$ vs $\theta_0$. It is noticed that for all the considered cases $|Z_4|$ displays an ascending behaviour in the first half of the interval and in leftover range the value of $|Z_4|$ decreases towards zero.

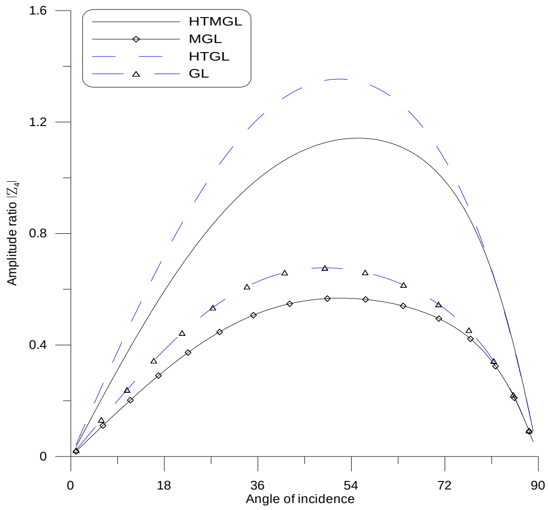


Fig. 9 Variation of amplitude ratio $|Z_4|$ for T- wave

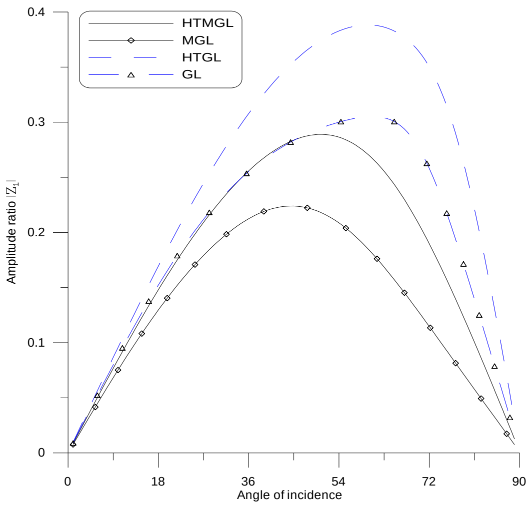


Fig. 10 Variation of amplitude ratio $|Z_1|$ for CD- I wave

**CD-I WAVE**

Fig. 10 which is a plot of $|Z_1|$ vs $\theta_0$. It is noticed that the value of $|Z_1|$ are greater for GL model of thermoelasticity i.e., HTGL and GL in comparison to those obtained for HTMGL and MGL.

Fig. 11 demonstrates $|Z_2|$ vs $\theta_0$. It is noticed that the values of $|Z_2|$ increases in the range $0^0 \leq \theta_0 \leq 40^0$, magnitude of values are higher in case of presence of HTT parameter for theories of thermoelasticity and values of $|Z_2|$ decreases in the remaining range.

Fig. 12 displays $|Z_3|$ vs $\theta_0$. It is observed that $|Z_3|$ for HTGL shows a steady state in the range $0^0 \leq \theta_0 \leq 55^0$, while for other considered cases $|Z_3|$ shows descending behaviour in the entire range except for MGL which shows increasing behaviour in $80^0 \leq \theta_0 \leq 90^0$.

Fig. 13 shows the variation of $|Z_4|$ vs $\theta_0$. It is observed that $|Z_4|$ exhibits identical behaviour across all considered cases. The values of $|Z_4|$ all found to be higher due to the influence of HTT

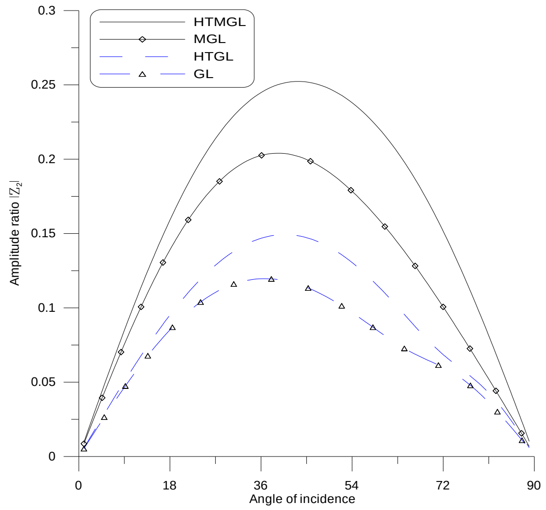


Fig. 11 Variation of amplitude ratio $|Z_2|$ for CD- I wave

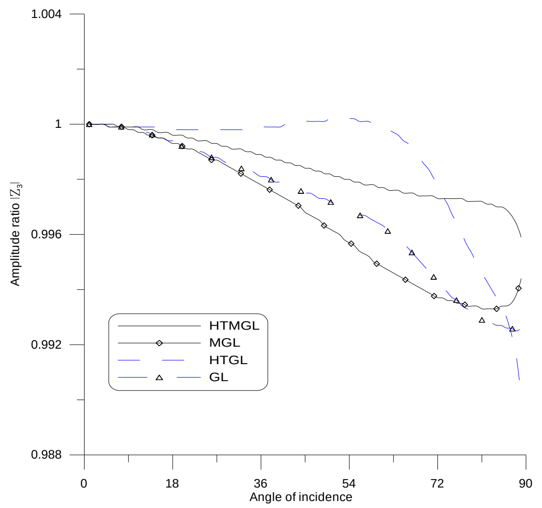


Fig. 12 Variation of amplitude ratio $|Z_3|$ for CD- I wave

parameter in both theories of thermoelasticity.

**CD-II WAVE**

Fig. 14 presents the variations of $|Z_1|$ vs $\theta_0$. It is observed that $|Z_1|$ follows a consistent trend across all cases in the entire range. In absence of the HTT parameter the values of $|Z_1|$ are greater for both theories of thermoelasticity. The maximum value of $|Z_1|$ occurs at $\theta = 45^0$ for G-L model of thermoelasticity, indicating its prominent behaviour compared to other model under consideration.

The trend of variations for variations of $|Z_2|$ vs $\theta_0$ is presented in Fig. 15. The graph reveals that $|Z_2|$ is higher for the HTMGL and MGL models in the entire range. This highlights the significance of different theories of thermoelasticity.

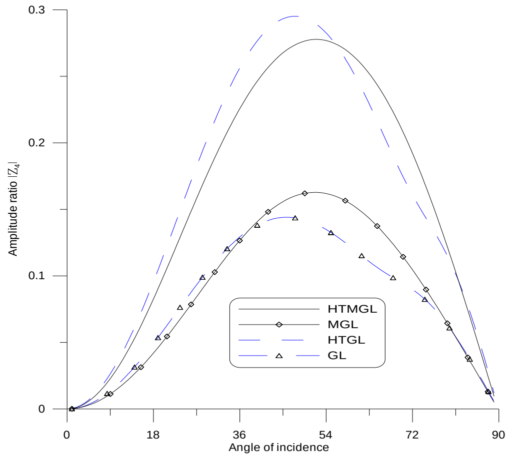


Fig. 13 Variation of amplitude ratio $|Z_4|$ for CD- I wave

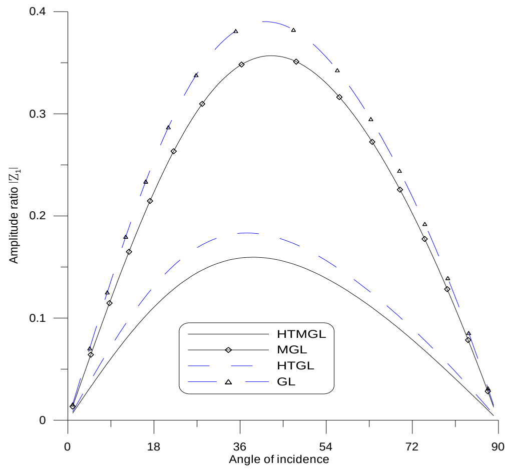


Fig. 14 Variation of amplitude ratio $|Z_1|$ for CD- II wave

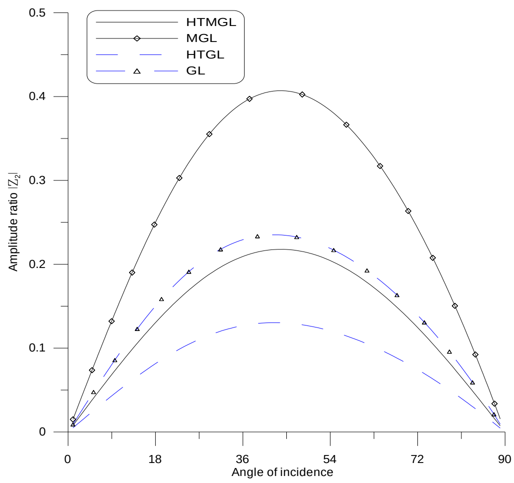


Fig. 15 Variation of amplitude ratio $|Z_2|$ for CD- II wave

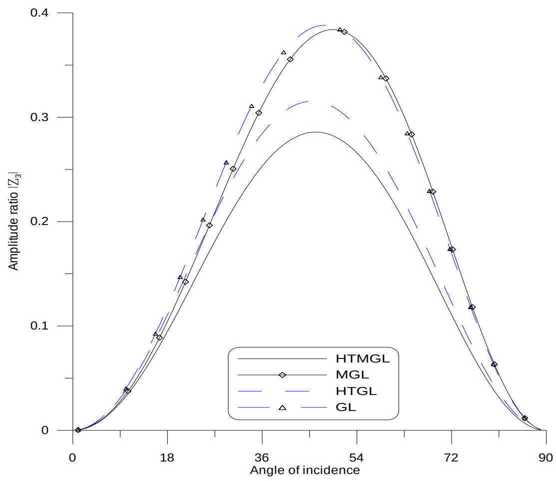


Fig. 16 Variation of amplitude ratio $|Z_3|$ for CD- II wave

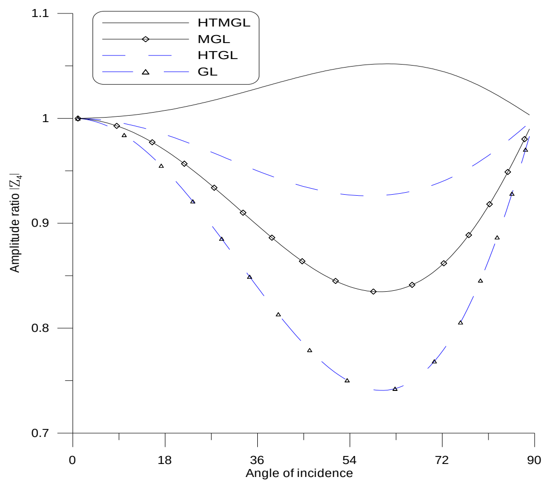


Fig. 17 Variation of amplitude ratio $|Z_4|$ for CD- II wave

Fig. 16 which is a plot of $|Z_3|$ vs $\theta_0$, it is noticed that initially $|Z_3|$ increases during the first half of interval and subsequently decreases in the remaining range. The magnitude of $|Z_3|$ is found to be higher for the G-L theory of thermoelasticity (HTGL and GL) compared to HTMGL and MGL.

Fig. 17, displays $|Z_4|$ vs $\theta_0$. It is noticed that $|Z_4|$ exhibits higher values in the presence of HTT parameter for both theories of thermoelasticity. The results indicate distinct difference in $|Z_4|$ which reveals that HTT parameter plays a significant role in influencing the amplitude ratio.

## 8. Conclusions

This investigation analyses an MMG-L generalized thermoelastic medium using the reflection technique. In this model the amplitude ratios of the four types of waves are determined namely

LD-wave, T-wave, CD-I wave and CD-II wave. For a two-dimensional problem the impact of HTT parameter along with different theories of thermoelasticity namely MG-L theory of thermoelasticity and G-L theory of thermoelasticity on amplitude ratios are investigated graphically. The following observations are noted:

1. The presence of HTT parameter significantly enhances the amplitude ratio for both theories of thermoelasticity. It is also noticed that $|Z_1|$ consistently increases, while $|Z_2|$ decreases towards zero for all considered cases. Both $|Z_3|$ and $|Z_4|$ display an initial rise followed by a decline indicating amplitude ratios are influenced by angle of incidence.
2. Both $|Z_1|$, $|Z_2|$ exhibits uptrend throughout the interval. The magnitude of $|Z_3|$ and $|Z_4|$ are notably higher for the G-L model of thermoelasticity compared to MG-L model.
3. It is noticed that $|Z_1|, |Z_2|$ and $|Z_4|$ increases initially but decreases with further increase in $\theta_0$. In contrast $|Z_3|$ shows a continuous decrease except for HTGL, which remain stable in most of the range. The HTT parameter plays a crucial role, enhancing the amplitude ratios in most cases.
4. It is noticed, CD-II waves demonstrate that $|Z_1|$, $|Z_2|$ and $|Z_3|$ increases during the first half of the interval but decreases later on. It is also noticed that the absence of HTT parameter amplifies the value of amplitude ratios, whereas $|Z_4|$ follows a declining trend, except for HTMGL which remain higher.

Though the problem is theoretical but the results are very useful for the researchers working in the field of seismology and earth crust drilling. Also, these findings contribute to the understanding of wave dynamics in thermoelastic media, with potential applications in seismology, material science, and engineering. Notably, such investigations play a vital role in hydrocarbon detection, mineral ore exploration.

## References

Abo-Dahab, S.M. and Lotfy, K. (2015), "Generalized magneto-thermoelasticity with fractional derivative heat transfer for a rotation of a fibre-reinforced thermoelastic", *J. Comput. Theor. Nanosci.*, **12**(8), 1869-1881. https://doi.org/10.1166/jctn.2015.3972.

Abo-Dahab, S.M., Lotfy, K. and Gohaly, A. (2015), "Rotation and magnetic field effect on surface waves propagation in an elastic layer lying over a generalized thermoelastic diffusive half-space with imperfect boundary", *Math. Prob. Eng.*, **2015**(1), 671783. https://doi.org/10.1155/2015/671783.

Abouelregal, A.E., Marin, M. and Alsharari, F. (2022), "Thermoelastic plane waves in materials with a microstructure based on micropolar thermoelasticity with two temperature and higher order time derivatives", *Math.*, **10**(9), 1552. https://doi.org/10.3390/math10091552.

El-Bary, A. (2021), "Hyperbolic two-temperature generalized thermoelasticity with fractional order strain of solid cylinder", *J. Eng. Therm. Sci.*, **1**(2), 30-42. https://doi.org/10.21595/jets.2021.21969.

El-Karamany, A.S. and Ezzat, M.A. (2004), "Analytical aspects in boundary integral equation formulation for the generalized linear micropolar thermoelasticity", *Int. J. Mech. Sci.*, **46**(3), 389-409. https://doi.org/10.1016/j.ijmecsci.2004.03.013

Eringen, A.C. (1966), "Linear theory of micropolar elasticity", *J. Math. Mech.*, 909-923.

Eringen, C. (1970), "Formulation of problems of micropolar elasticity", *Foundations of Micropolar Thermoelasticity: Course held at the Department for Mechanics of Deformable Bodies July*, **1970**, 87-102. https://doi.org/10.1007/978-3-7091-2904-3_4.

Ezzat, M.A. (1995), "Fundamental solution in thermoelasticity with two relaxation times for cylindrical regions", *Int. J. Eng. Sci.*, **33**(14), 2011-2020. https://doi.org/10.1016/0020-7225(95)00050-8.

Ezzat, M.A. (2004), "Fundamental solution in generalized magneto-thermoelasticity with two relaxation times for perfect conductor cylindrical region", *Int. J. Eng. Sci.*, **42**(13-14), 1503-1519. https://doi.org/10.1016/j.ijengsci.2003.09.013.

Ezzat, M.A. and Awad, E.S. (2009), "Micropolar generalized magneto-thermoelasticity with modified Ohm's and Fourier's laws", *J. Math. Anal. Appl.*, **353**(1), 99-113. https://doi.org/10.1016/j.jmaa.2008.11.058.

Ezzat, M.A., El-Karamany, A.S. and El-Bary, A.A. (2018), "Two-temperature theory in Green–Naghdi thermoelasticity with fractional phase-lag heat transfer", *Microsyst. Technol.*, **24**, 951-961. https://doi.org/10.1007/s00542-017-3425-6.

Ezzat, M.A., El-Karamany, A.S. and Ezzat, S.M. (2012), "Two-temperature theory in magneto-thermoelasticity with fractional order dual-phase-lag heat transfer", *Nucl. Eng. Des.*, **252**, 267-277. https://doi.org/10.1016/j.nucengdes.2012.06.012.

Gauthier, R.D. (1982), "Experimental investigations on micropolar media", *Mech. Microp. Media*, 395-463. https://doi.org/10.1142/9789812797247_0007.

Green, A.E. and Lindsay, K. (1972), "Thermoelasticity", *J. Elast.*, **2**(1), 1-7. https://doi.org/10.1007/BF00045689.

Kaushal, S., Kumar, R., Kaur, K. and Sharma, G. (2023), "A Mathematical model for the deformation problem in a generalized thermoelastic medium under modified Green–Lindsay mode", *Int. Appl. Mech.*, **59**(6), 742-753. https://doi.org/10.1007/s10778-024-01257-x.

Kumar, R., Kaur, M. and Rajvanshi, S.C. (2015), "Representation of fundamental and plane waves solutions in the theory of micropolar generalized thermoelastic solid with two temperatures", *J. Comput. Theor. Nanosci.*, **12**(4), 691-702. https://doi.org/10.1166/jctn.2015.4146.

Kumar, R., Kaushal, S. and Kochar, A. (2022), "Response of impedance parameters on waves in the micropolar thermoelastic medium under modified Green-Lindsay theory", *ZAMM-J. Appl. Math. Mech./Zeitschrift für Angewandte Mathematik und Mechanik*, **102**(9), e202200109. https://doi.org/10.1002/zamm.202200109.

Kumar, R., Prasad, R. and Kumar, R. (2020), "Thermoelastic interactions on hyperbolic two-temperature generalized thermoelasticity in an infinite medium with a cylindrical cavity", *Eur. J. Mech.-A/Solid.*, **82**, 104007. https://doi.org/10.1016/j.euromechsol.2020.104007.

Lord, H.W. and Shulman, Y. (1967), "A generalized dynamical theory of thermoelasticity", *J. Mech. Phys. Solid.*, **15**(5), 299-309. https://doi.org/10.1016/0022-5096(67)90024-5.

Lotfy, K. (2012), "Mode-I crack in a two-dimensional fibre-reinforced generalized thermoelastic problem", *Chin. Phys. B*, **21**(1), 014209. https://doi.org/10.1088/1674-1056/21/1/014209.

Lotfy, K. and Tantawi, R.S. (2020), "Photo-thermal-elastic interaction in a functionally graded material (FGM) and magnetic field", *Silicon*, **12**(2), 295-303. https://doi.org/10.1007/s12633-019-00125-5.

Lotfy, K., El-Bary, A.A. and Tantawi, R.S. (2019), "Effects of variable thermal conductivity of a small semiconductor cavity through the fractional order heat-magneto-photothermal theory", *Eur. Phys. J. Plus*, **134**(6), 280. https://doi.org/10.1140/epjp/i2019-12631-1.

Lotfy, K., Elidy, E.S. and Tantawi, R.S. (2021), "Piezo-photo-thermoelasticity transport process for hyperbolic two-temperature theory of semiconductor material", *Int. J. Modern Phys. C*, **32**(07), 2150088. https://doi.org/10.1142/S0129183121500881.

Mahdy, A.M.S., Gepreel, K.A., Lotfy, K. and El-Bary, A.A. (2021), "A numerical method for solving the Rubella ailment disease model", *Int. J. Modern Phys. C*, **32**(07), 2150097. https://doi.org/10.1142/S0129183121500972.

Mahdy, A.M.S., Mohamed, M.S., Lotfy, K., Alhazmi, M., El-Bary, A.A. and Raddadi, M.H. (2021), "Numerical solution and dynamical behaviors for solving fractional nonlinear Rubella ailment disease model", *Result. Phys.*, **24**, 104091. https://doi.org/10.1016/j.rinp.2021.104091.

Marin, M., Öchsner, A. and Bhatti, M.M. (2020), "Some results in Moore-Gibson-Thompson thermoelasticity of dipolar bodies", *ZAMM-J. Appl. Math. Mech./Zeitschrift für Angewandte Mathematik und Mechanik*, **100**(12), e202000090. https://doi.org/10.1002/zamm.202000090.

Quintanilla, R. (2018), "Some qualitative results for a modification of the Green–Lindsay thermoelasticity", *Meccanica*, **53**(14), 3607-3613. https://doi.org/10.1007/s11012-018-0889-0 3607-3613.

Sarkar, N. and Mondal, S. (2020), "Thermoelastic plane waves under the modified Green–Lindsay model with two-temperature formulation", *ZAMM-J. Appl. Math. Mech./Zeitschrift für Angewandte Mathematik und Mechanik*, **100**(11), e201900267. https://doi.org/10.1002/zamm.201900267.

Sherief, H.H. and Hussein, E.M. (2023), "Fractional order model of micropolar thermoelasticity and 2D half-space problem", *Acta Mechanica*, **234**(2), 535-552. https://doi.org/10.1007/s00707-022-03399-w.

Tauchert, T.R., Claus Jr, W.D. and Ariman, T. (1968), "The linear theory of micropolar thermoelasticity", *Int. J. Eng. Sci*., **6**(1), 37-47. https://doi.org/10.1016/0020-7225(68)90037-2.

Vlase, S., Marin, M., Scutaru, M.L. and Munteanu, R. (2017), "Coupled transverse and torsional vibrations in a mechanical system with two identical beams", *AIP Adv*., **7**(6), https://doi.org/10.1063/1.4985271.

Youssef, H.M. (2006), "Theory of two-temperature-generalized thermoelasticity", *IMA J. Appl. Math*., **71**(3), 383-390. https://doi.org/10.1093/imamat/hxh101.

Youssef, H.M. and Al-Lehaibi, E.A. (2022), "2-D mathematical model of hyperbolic two-temperature generalized thermoelastic solid cylinder under mechanical damage effect", *Arch. Appl. Mech.*, **92**(3), 945-960. https://doi.org/10.1007/s00419-021-02083-0.

Youssef, H.M. and El-Bary, A.A. (2018), "Theory of hyperbolic two-temperature generalized thermoelasticity", *Mater. Phys. Mech*., **40**(2), 158-171. https://doi.org/10.18720/MPM.4022018_4.

Yu, Y.J., Xue, Z.N. and Tian, X.G. (2018), "A modified Green–Lindsay thermoelasticity with strain rate to eliminate the discontinuity", *Meccanica*, **53**, 2543-2554. https://doi.org/10.1007/s11012-018-0843-1.